Link Budget and Antenna Design for an AESA in the FR2 n512 Bands

***Abstract*— Active Electronic Scanned Array (AESA) systems will form the backbone of future 5G NR systems operating in the FR2 n512 bands, making careful design of the various system blocks a priority. In this work, the link budget for the uplink and downlink of an ESA system has been evaluated both analytically and using the VSS software available within the AWR Cadence tool. The same tool has been also used to evaluate the radiation patterns of the antenna array used in the AESA. The EIRP and G/T values found were higher than those proposed in the literature, indicating the importance of accurate link budget evaluation to ensure the best system performance.**

***Keywords*— Antenna, EIRP, EVM, G/T, link budget, phased array, 64-QAM.**

I. Introduction

Currently, satellite telecommunications (broadcasting TV and Internet) use geostationary satellites (GEO) about 36,000 km away from the Earth or low Earth orbit (LEO) satellites at altitudes between 500 and 700 km. The main advantages of LEO satellite systems are a more extended coverage of the surface of the Earth that permits the availability of satcom links in areas not served by GEO systems; a reduced latency (less than 2 ms) that proves to be fundamental for real-time applications; and a reduced size of the user terminals due to the reduced path loss of low-orbit satellites.

However, the benefits given by LEO satellites come with technical challenges. LEO satellites travel at high speed and can ensure the coverage of the targeted areas of the Earth's surface only for a limited time, placing stringent requirements on the antenna for both the space and ground segment. In particular, the antennas should be agile and able to steer their main beam over a large field of view. For LEO non-terrestrial networks, the European Telecommunications Standards Institute (ETSI) has established the 27.5-30 GHz band for the uplink and the 17.3-20.2 GHz band for the downlink (FR2 n512 denomination) [1].

Some LEO constellations are already in use and represent the complement of the nascent 5G infrastructure of land that will become the exclusive means for the control and communication of maritime and ocean areas. Moreover, satellite telecommunications have a potentially huge market of commercial applications, industrial as well as surveillance and monitoring of civil infrastructure. There are also specific fields of application, such as advanced driver assistant (ADAS) 5G systems or road-side assistance, which find in the LEO space domain their primary form of evolution [2].

The aim of this study is the design of an active electronically scanned array (AESA) system operating in the FR2 n512 frequency bands. To this purpose, first the system link budget will be analytically investigated and then implemented within the VSS software available inside the tool AWR by Cadence. Then a possible configuration for the antenna array will be investigated.

II. Link Budget Calculations

The typical block diagram for a ground to satellite uplink is reported in Fig. 1, where upper blocks are located on the ground terminal while lower blocks are in the satellite one. In Fig. 1 only one beamformer is shown while, in practical cases, all the antennas of the array are driven by a beamformer followed by a power amplifier. Fig. 2 shows the block diagram of the satellite to ground downlink where upper blocks are located on the satellite terminal while lower blocks are in the ground one. In this case, at the output of each antenna there is a low noise figure amplifier.

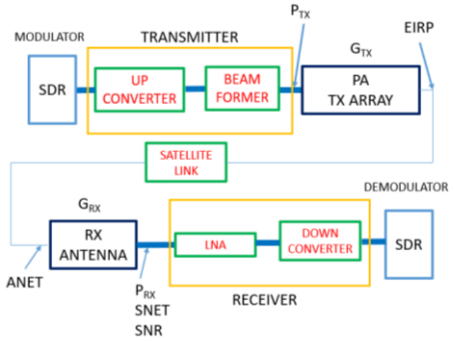

Fig. 1. Block diagram for the ground to satellite uplink (27.5 – 30 GHz).

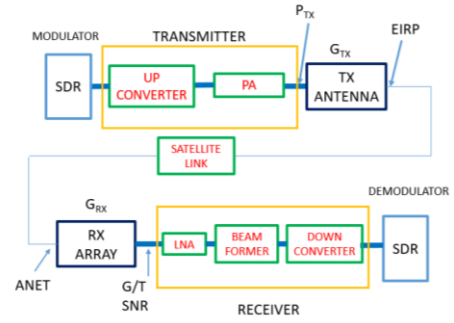

Fig. 2. Block diagram for the satellite to ground downlink (17.3 – 20.2 GHz).

The Signal to Noise ratio (SNR) at the input of the receiver is a fundamental metric in link budget calculations. The minimum acceptable SNR depends on the modulation scheme used and on the minimum acceptable Block Error Rate (BLER). At low SNR values, QPSK modulation can be used, whereas at higher SNR values, modulation schemes up to 1024-QAM can be adopted. For example, to use 64-QAM modulation with Modulation and Coding Scheme 14 and BLER=10^{-1} requires a received SNR of at least 17 dB [3].

Concerning the uplink, the reference parameter in the transmitting system is the effective isotropically radiated power (EIRP). It is defined as:

$$EIRP_{dBm} = P_{TXdBm} + G_{TXdB} \quad (1)$$

where P_{TXdBm} is the transmitted power and G_{TXdB} is the gain of the transmitting antenna.

The received power P_{RXdBm} is given by:

$$P_{RXdBm} = EIRP_{dBm} + G_{RXdB} - L_{FSdB} - L_{RAINdB} - L_{ATMdB} \quad (2)$$

where G_{RXdB} is the gain of the receiving antenna, L_{FSdB} is the free space attenuation, L_{RAINdB} is the rainfall attenuation, L_{ATMdB} is the atmosphere attenuation.

The main power loss in satellite links is due to the path, called free-space loss that is given by:

$$L_{FSdB} = 20log_{10}(4\pi\, d_{sp}/\lambda) \quad (3)$$

where

$$d_{sp} = r_e\left(\sqrt{(r_e + d)^2/r_e^2 - cos(\theta_{el})^2} - sin(\theta_{el})\right) \quad (4)$$

is the satellite effective path, θ_{el} is the elevation angle in degrees, r_e is the radius of the Earth and d_{sp} is the max orbit distance.

The attenuation introduced by the atmospheric gases and atmospheric attenuation were calculated using equations reported in the "ITU-R P.676-13" recommendation [4]. This returns the value $L_{ATMdB} = 0{,}21\, dB$. Therefore for the atmospheric attenuation a conservative value of $L_{ATMdB} = 0{,}5\, dB$ will be considered. Scintillation effect and Faraday rotation are negligible for signals above 10 GHz and will therefore not be considered in this analysis. Attenuation due to rainfall is also very important, and according to the Glossary of Meteorology of the American Meteorological Society [5], a value of 5 mm/h of "moderate" rain was selected. Then, according to ITU-R P.838-3 [6] tables, an attenuation of 1 *dB/km* at 30 GHz was chosen. Finally, multiplying this value for the distance the signal travels inside the rain layer, assumed to have a thickness of 3 km, which is an approximation of the height of most rain-producing clouds, and considering the slant path due to the 50 degrees of elevation angle, the effective path is about 3.9 km, and a value of 4 dB was fixed to guarantee a slight margin of safety.

The calculation of the System Noise Equivalent Temperature (SNET) at the input of the receiver is then carried out. In addition to the antenna noise equivalent temperature (ANET), the contribution of the noise figure (NF) of the low noise amplifier and the attenuation introduced by the cables connections (L_{RX}) are also taken into account giving:

$$SNET = ANET + RPT \cdot \left(10^{\frac{NF+L_{RX}}{10}} - 1\right) \quad (5)$$

where RPT is the Receiver Physical Temperature.

The signal to noise ratio at the receiver input is given by:

$$SNR_{dB} = P_{RXdBm} - N_{dBm} \quad (6)$$

where the noise power in dBm is:

$$N_{dBm} = 10log_{10}(kBT) + 30 \quad (7)$$

where B is the noise bandwidth of the receiver, k is the Boltzmann constant equal to $1{,}38 \cdot 10^{-23}[W \cdot Hz^{-1} \cdot K^{-1}]$, T is the temperature in Kelvin, and the value of SNET will be used for T.

If Na is the number of antennas in the uplink transmitting system with gain G_{AdB} and P_{AdBm} is the output power of the amplifier that powers the antennas, it holds:

$$P_{AdBm} = EIRP_{dBm} - G_{AdB} - 20log_{10}(Na) \quad (8)$$

where the term $20log_{10}(Na)$ is due to the sum of the array factor ($10log_{10}(Na)$) and of the overall power supplied to the Na antennas ($10log_{10}(Na)$).

With reference to the downlink, a typical figure of merit in the receiving system is the gain over temperature ratio defined as:

$$G/T_{dB/K} = SNR_{dB} - EIRP_{dBm} + L_{FSdB} + L_{RAINdB} + L_{ATMdB} + 10log10(KB) \quad (9)$$

or:

$$G/T_{dB/K} = G_{AdB} + 20log10(Na) - 10log10(\text{SNET}) \quad (10)$$

Moreover, from (5) the receiver noise figure is:

$$NF = 10\text{log}10(1 + (\text{SNET} - ANET)/RPT) - L_{RX} \quad (11)$$

Concerning the uplink, the Noise Figure (*NF*) of the LNA and the losses in the satellite receiver (L_{RX}) are considered to be 2.8 dB and 1.6 dB, respectively [7]. For an antenna on the satellite looking down at Earth ANET is 290 *K* while *RPT* is considered equal to 275 K. The resulting *SNET* (with B = 10 MHz) is calculated to be around 968,5 K giving rise to a noise power N_{dBm}= -98.7 dBm. As evidenced before, the minimum SNR needed for the 64 QAM modulation is 17 dB. Consequently, the power that must be received is about P_{RXdBm} = -81.7 dBm. Considering a maximum transmitter-receiver distance of 800 km, a centre frequency of 28.75 GHz, a receive gain of G_{RXdB}=20dB [8]-[9] and the above found values for atmospheric, rain, and cable attenuation, we find that an $EIRP_{dBm}$ = 82 dBm is required that correspond to 52 dBW. This $EIRP_{dBm}$ value can be obtained with various values of the number of antennas (Na), the gain of the single antenna (G_{AdB}) and the power applied to the antenna (P_{AdBm}). Some combinations are reported in Table I.

Table I. Combinations of number of antennas, antenna gain and amplifier power that give rise to the requested $EIRP_{dBm}$

	Na	G_{AdB}	P_{AdBm}	PA (W)
1	8×8 = 64	15	31	1.2
2	10×10 = 100	15	27	0.5
3	16×16 = 256	5	29	0.8
4	20×20 = 400	5	25	0.35

In particular, the configuration reported in row 1 of Table I can be obtained using a rectangular array of 64 horn antennas with a gain of approximately 15 dBi and a 31 dBm PA. Similarly, the one in row 4 considering a rectangular array of 400 patch antennas with 5 dBi gain driven by a 25 dBm PA.

With reference to the downlink, P_{TXdBm} = 36 dBm and G_{TXdB}=20 dB have been assumed [9] and, as before, SNR= 17 dB. In this way by (9) we get a receiver gain over temperature ($G/T_{dB/K}$) value of 10.3. As for the uplink, after selecting the number of antennas (Na) the antenna gain (G_{AdB}), the receiver equivalent temperature is achieved by inverting (10). In the case considered for the downlink, RPT = 290 K and for ANET a value of 35 K was extracted from the graph in [10]. Table II shows for various combination of Na and G_{AdB} the corresponding maximum NF value achieved with (11).

Table II. Combinations of number of antennas, antenna gain and LNA noise figure that give rise to the requested $G/T_{dB/K}$.

	Na	G_{AdB}	NF [dB]
1	8×8 = 64	15	< 13.6
2	6×6 = 36	15	< 8.8
3	16×16 = 256	5	< 15.6
4	8×8 = 64	5	< 4.4

III. Power Budget Simulations

The designed AESA system has been implemented inside the software VSS available within the tool AWR by Cadence. This tool allows to apply a modulated signal at the AESA input and to investigate the received signal at the output of the chain (see Fig. 3). The system parameter for the uplink together with the data reported in the first row of Table I were implemented. The achieved power budget along the system test point in Fig. 3 is reported in Fig. 4 (a) together with the simulated noise spectral power density.

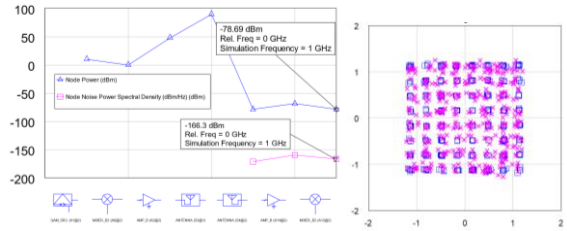

(a) (b)

Fig. 4. Power budget for the AESA uplink (a) and I/Q plot for a 64 QAM modulation

By considering the chosen 10 MHz bandwidth, the SNR at the receiver input is 17 dB as per specification. The constellation diagram for a 64 QAM modulation is reported in Fig. 4(b) and an EVM of about 10% has been simulated by the VSS software.

IV. Antenna Array Design

To realize the system reported in the first row of Table I circularly polarized antennas with 15 dB gain are necessary. This specification can be fulfilled by using horn antennas. The chosen dual polarization antenna geometry and dimensions are reported in Fig. 5. Both the feeding structure and the horn have a square section. Two transversal sections are outlined in Fig. 5 with a view of the coaxial to waveguide transition.

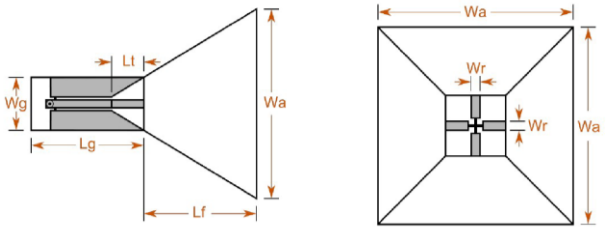

Fig. 5 Horn antenna geometry. Wa = 19 mm, Wg = 6.5 mm, Wr = 1.15 mm, Lg = 17 mm, Lf = 30 mm

The antenna has been studied with the CST software and the reflection coefficient and realized gain as a function of frequency are reported in Fig. 6 (a) and (b), respectively. The figures show a reflection coefficient at both ports of the antenna lower than -10 dB in the 27.5-30 GHz band with a realized gain between 14.3 and 15.2 dBi. The simulated axial ratio was between 1.4 and 1.8 dB. This antenna is under production by utilizing additive manufacturing by 3D printing, and subtractive manufacturing in order to compare the two approaches.

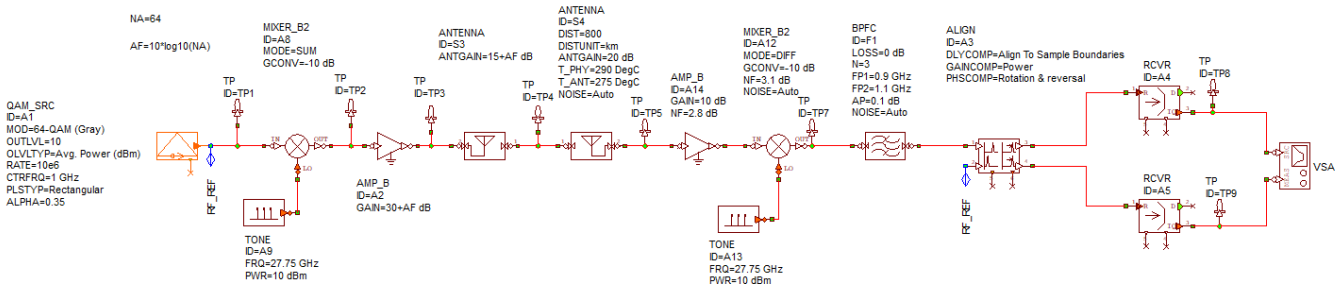

Fig. 3. Block diagram of the AESA uplink.

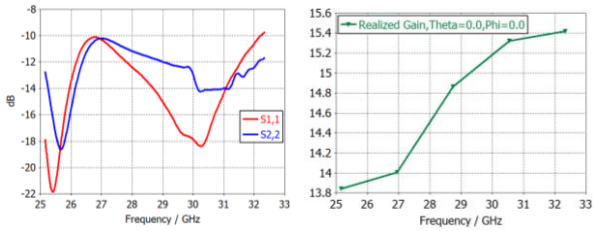

(a) (b)

Fig. 6. Antenna reflection coefficient at port 1 and port 2 (a) and antenna realized gain (b).

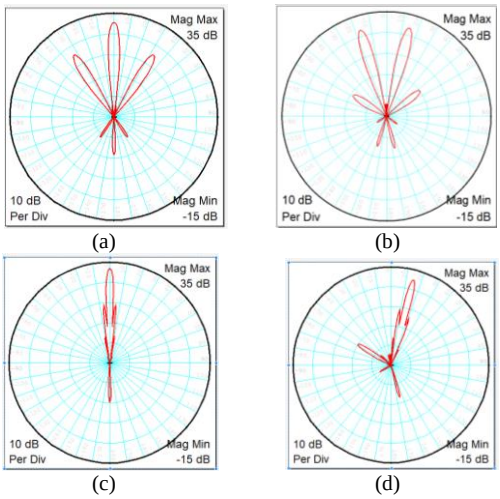

(a) (b)

(c) (d)

Fig. 7. Radiation pattern of a rectangular array without steering (a) and with 15° steering (b). Radiation pattern of a 60° tilted triangular array without steering (c) and with 15° steering (d).

Finally, the horn antenna radiation pattern simulated with the CST software has been imported inside the VSS tool and the radiation pattern of a 8 × 8 rectangular array (1.8 λ spaced at 28.75 GHz) has been evaluated. Fig. 7(a) and Fig. 7(b) show the radiation patterns without and in the presence of a 15° steering, respectively. Grating lobes at ± 30 degrees with respect to the main beam are observed. Then a triangular array (1.8 λ spaced) with 60° angle between x-y axes has been studied [12]. Fig. 7(c) and Fig. 7(d) show the radiation patterns without and in the presence of a 15° steering, respectively. In this case a reduction in the grating lobe amplitude and an increase in the grating lobe free region is evidenced. Moreover, the triangular array gives rise to gains of 31.9 and 29.9 dBi with 0° and 15 ° steering, respectively, with an increase of about 1.5 dB with respect to the rectangular array.

V. Conclusion

The analysis conducted in this work has highlighted that to guarantee 17 dB of SNR an EIRP of 82 dBm and a G/T of at least 10 dB/K are necessary for a LEO uplink and down link, respectively. These values can be achieved with various combinations of array antenna number, amplifiers gain and noise figure. EIRP and G/T values are slightly higher than those proposed in the literature [11], indicating the need to conduct detailed analyses to guarantee the services of the new 5G NR systems.

References

[1] ETSI TS 138 101-5 V 18.7.0 2024 10, 5G; NR; User Equipment (UE) radio transmission and reception; Part 5: Satellite access Radio Frequency (RF) and performance requirements (3GPP TS 38.101-5 version 18.7.0 Release 18).

[2] C. Sacchi, T. Rossi, M. Murroni and M. Ruggieri, "Extremely High Frequency (EHF) Bands for Future Broadcast Satellite Services: Opportunities and Challenges," IEEE Transactions on Broadcasting, vol. 65, no. 3, pp. 609-626, Sept. 2019.

[3] L. Méndez-Monsanto, A. Mac Quarrie, M. R. Ghourtani, M. J. López Morales, A. G. Armada and A. Burr, "BLER-SNR Curves for 5G NR MCS under AWGN Channel with Optimum Quantization," 2024 IEEE 100th Vehicular Technology Conference, Washington, DC, USA, 2024, pp. 1-6.

[4] Recommendation ITU-R P.676-13, Attenuation by atmospheric gases and related effects. 08, 2022.

[5] https://web.archive.org/web/20100725142506/http://amsglossary.allenpress.com/glossary/ search?id=rain1.

[6] Recommendation ITU-R P.838-3 1, Specific attenuation model for rain for use in prediction methods.

[7] https://www.analog.com/media/en/technical-documentation/data-sheets/hmc751.pdf.

[8] M. Uko, M. Zafar, A. Altaf, S. Udeshi, S. Ekpo, B. Adebisi, "K/Ka-band transceiver sensitivity modeling and link characterization for integrated 5G-LEO", 37th International Communications Satellite Systems Conference (ICSSC-2019), Okinawa, Japan, 24 March 2021.

[9] M. Jefferies, K. Maynard, P. Garner, J. Mayock, P. Deshpande,"26-GHz Data Downlink and RF Beacon for LEO In Orbit Demonstrator Satellite", Int, Workshop on Tracking, Telemetry and Command Systems for Space Applications (TTC), Noordwijk, Netherlands, 13-16 September 2016.

[10] B. Hsu, "Phase array antenna G/T measurement," Rohde&Schwarz application note.

[11] S. Muralidharan and S. S. Deo, "Flat panel AESAs for SATCOM links: Design and array synthesis," 2022 IEEE International Symposium on Phased Array Systems & Technology (PAST), Waltham, MA, USA, 2022, pp. 01-05.

[12] S. R. Zinka, I. -B. Jeong, J. -H. Chun and J. -P. Kim, "A Novel Geometrical Technique for Determining Optimal Array Antenna Lattice Configuration," in *IEEE Transactions on Antennas and Propagation*, vol. 58, no. 2, pp. 404-412, Feb. 2010.